

Enriching solar-cell front electrodes with Ag@MgO nanoparticles via physical deposition: A morphological and optical investigation

M. CALEFFI(*) and A. TONELLI

Department of Physics, University of Modena and Reggio Emilia - Modena, Italy

received 8 February 2022

Summary. — Core-shell metal-oxide nanoparticles (NPs) have been extensively exploited in Perovskite solar cells (PSCs) to improve light harvesting and power conversion efficiency. Herein, we exploit a sequential physical method based on nanocluster magnetron-sputtering techniques and MgO deposition to grow Ag NPs—embedded in an ultrathin MgO matrix—on top of a multilayered substrate, which acts as a front electrode in PSCs. The overall system morphology is investigated by Scanning Electron Microscopy (SEM) for different Ag@MgO coverages. The optical reflectance (R) and transmittance (T) spectra of both pristine and functionalized multilayer substrates are acquired for different substrate batches, showing remarkable differences. Data are analyzed by a specifically designed fitting procedure, which evaluates the contribution to R and T of each layer and extracts their complex refractive index \tilde{n} , as well as their morphological properties, *i.e.* their thickness and roughness.

1. – Introduction

In the past decade, plasmonic metal nanoparticles (NPs) have been extensively exploited in association with photo-active materials, to enhance device performance in solar energy conversion applications [1, 2], and in particular in Perovskite Solar Cells (PSCs) [3, 4]. Metal-based core-shell NPs are nanostructures (NS) composed of an inner core (in this case, Silver) and an outer shell made of a different material (*e.g.* metals, metal oxides or even organic materials) [3, 5]. Their optical and electronic properties may be tuned by varying both core and shell materials, as well as the ratio between their radii. The shell—surrounding the NP core and therefore isolating it from the external environment—is essential in photovoltaic applications, as it shields the core from unwanted phenomena, *e.g.* NP aggregation [6], chemical oxidation [7], and thermal degradation. Recently, it has been highlighted that the substrate may influence the morphology of deposited NPs [8], and—in turn— their overall NP optical activity. In this work, we exploit a magnetron-based nanocluster source [9] to synthesise and deposit

(*) Corresponding author. E-mail: matteo.caleffi@unimore.it

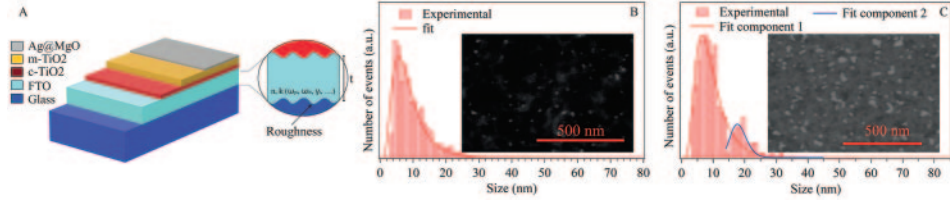


Fig. 1. – SEM - (A) multilayer architecture; NP size distribution along with the BSE image of Ag@MgO NPs on the m-TiO₂ layer for coverage (B) 1.5% and (C) 6%.

Ag@MgO NPs on top of Glass/FTO/TiO₂ substrates —as depicted in fig. 1(A)— which act as front electrodes in PSCs [10]. This physical deposition method —as compared to the more widely used chemical approaches— provides versatility in the choice of core and shell materials, and guarantees precise control over the NP size distribution as well as the absence of solvents. In order to establish the effective role played by the NPs in the PSC efficiency, it is crucial to preliminarily investigate their morphological and optical properties on actual substrates. We therefore focus our attention on the characterization of both the pristine and the functionalized substrates, in terms of morphology and optical features. We develop a specifically designed procedure which exploits the optical transfer matrix method [11] to reproduce the experimental R and T optical spectra. As we shall discuss in more detail in the Results section, our approach somewhat differs from other strategies reported in literature and allows us to estimate both the actual dielectric function and the surface roughness and thickness of each layer.

2. – Experimental

The multilayer substrates comprise a TiO₂ mesoporous (m-TiO₂) layer (120 nm nominal thickness), deposited on top of a c-TiO₂ layer (50 nm), grown on commercial Glass/FTO substrates, as detailed in [12]. Ag@MgO NP synthesis was carried out in a UHV chamber. The Ag NPs and MgO layer were deposited on m-TiO₂ substrates and their deposition was performed using a nanocluster source [12,13]. The NP morphology was investigated by SEM (Nova Nano SEM450, FEI Company-Bruker Corporation) with a Schottky field-emission gun (SFEG). The optical experiments were recorded ex situ with a linearly polarized s-radiation, with an angle of 45° between specimen and incident light, by means of an Ocean Optics DH-20000-BAL light source [12].

3. – Results and discussion

The morphology of Ag@MgO NPs deposited on m-TiO₂ is investigated by SEM by collecting the backscattered electron signal, which provides chemical-sensitive contrast. In figs. 1(B) and (C), the surface micrographs corresponding to NP coverage of 1.5% and 6%, respectively, are reported, along with the corresponding NP size distribution. For the lowest coverage, the distribution is fitted with a single log-normal component [14], centered at an NP mean diameter of 8 nm. For the higher coverage, a bimodal distribution is observed; the first component (red solid line) is still centered at 8 nm and associated to isolated NPs, while the second one (blue line), corresponding to a NP mean diameter of about 17 nm, is due to the coalescence of NPs.

As shown in fig. 1(A), the front electrode of a PSC is characterized by a multilayer structure, where each layer contributes to light reflection, transmission, diffusion and ab-

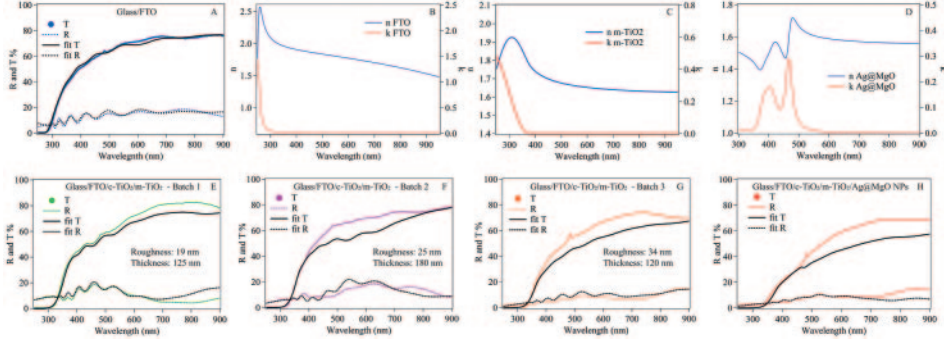


Fig. 2. – (A) R and T spectra overlapped with their respective fit curves for Glass/FTO system. n and k indices for (B) Glass/FTO, (C) Glass/FTO/ c -TiO₂/ m -TiO₂, and (D) Ag@MgO NP systems, extracted from the fitting procedure. The dielectric functions for Ag and MgO are taken from literature [16]. R and T spectra (experimental and fit) for (E)–(G) the Glass/FTO/ c -TiO₂/ m -TiO₂ system for three different batches, and (H) Ag@MgO NPs.

sorption. The interpretation of optical spectra is therefore not straightforward and needs accurate modelling. Our approach is based on the optical transfer matrix method [11] and fits the experimental R and T spectra using parametric models of dielectric functions, appropriate for each layer. Following [11], we use modified Fresnel coefficients obtained by introducing a Gaussian factor which accounts for partial coherence due to interface roughness. In this way, the results of the fitting procedure are i) the thickness and roughness of each layer, ii) their actual complex refractive indices —which may significantly differ from those of bulk, ideal materials typically used in other approaches [13]. At variance with the approach reported in [15], the use of model dielectric functions ensures the physical soundness of our results, which *a priori* satisfy the Kramers-Kronig relations.

Initially, as shown in fig. 2(A), we measured and analyzed the simpler Glass/Fluorine-Doped Tin Oxide (FTO) system; the remarkable agreement between experiments and fitting is obtained using a Drude-Lorentz model [17] for the FTO complex refractive index (fig. 2(B)). In figs. 2(E)–(G), the optical spectra of different batches of the complete glass/FTO/ c -TiO₂/ m -TiO₂ multilayer are reported along with the corresponding fits; while all curves display the same R and T onset at 300 nm, the R and T intensity, as well as their wavelength-dependent modulation vary remarkably among different batches. To fit these spectra, we use the pre-determined FTO parameters, and model the c - and m -TiO₂ dielectric functions with the Tauc-Lorentz [18] and Bruggeman models [19], respectively. For the latter, we considered the porosity of the m -TiO₂ layer as spherical inclusions of air (average dimension of pores is about 30–40 nm). The fitting curves — corresponding to the m -TiO₂ refractive index shown in fig. 2(C)— are in fair agreement with the experiment. In particular, we noted the differences between batches are reproduced by varying only the roughness and thickness of the mesoporous layer, while all other parameters are kept fixed. Finally, fig. 2(H) shows the T and R spectra for the NP functionalized substrate; comparison with the spectra of the pristine multilayer (fig. 2(G)) shows a considerable decrease in R and T intensity in the range 350–550 nm, while no sharp plasmonic feature can be observed. The fitting curves are obtained by adding a 5 nm Ag@MgO layer, using the Maxwell-Garnett model [20] (fig. 2(E)), where MgO and Ag NPs represent the embedding matrix and the elliptical inclusions, respectively, with a volume fraction of 2% (in agreement with SEM analysis of 1.5%). The intensity decrease

observed in fig. 2(H) can only be fitted by increasing the roughness of the interface between the c- and m-TiO₂ layers. This can be seen as an effective parameter describing the increase of light scattering produced by the Ag NPs inside the m-TiO₂ layer.

4. – Conclusions

In this work, we exploited the magnetron sputtering method to deposit Ag@MgO NPs on top of m-TiO₂ substrates used in PSCs, investigating their morphological and optical properties. SEM provides information on the NP lateral size distributions and shows coalescence taking place for coverages around 6% of Ag. The optical spectra fitting provides both the complex refractive indices and the thickness and roughness of each layer. In particular, optical spectra from different m-TiO₂ batches are reproduced by varying the thickness of the m-TiO₂ layer, showing that optical analysis provides an effective tool to monitor the growth parameters of these multilayer substrates, for quality control purposes. Furthermore, adding the Ag@MgO NPs decreases the R and T intensity, which can be reproduced by an effective increase in the m-TiO₂ layer roughness. On the other hand, no clear fingerprint of the plasmonic loss can be observed in the spectra, possibly due to both the small amount of added NPs and to the broadening of the plasmonic feature, caused by the NP ellipsoidal shape.

* * *

We gratefully thank A. Agresti, P. Mariani, S. Pescetelli, and A. Di Carlo (CHOSE, University of Tor Vergata) for providing the substrates; L. Pasquali, V. De Renzi, and S. D’Addato (University of Modena and Reggio Emilia) for providing materials, laboratory facilities and thought-provoking discussions.

REFERENCES

- [1] ASTRUC D., *Nanoparticles and Catalysis* (Wiley-VCH) 2008.
- [2] DERKACS D. *et al.*, *Appl. Phys. Lett.*, **9** (2006) 093103.
- [3] SALIBA M. *et al.*, *Adv. Funct. Mater.*, **25** (2015) 5038.
- [4] YAO K. *et al.*, *ACS Nano*, **13** (2019) 5397.
- [5] DONG H. *et al.*, *Org. Electron.*, **60** (2018) 1.
- [6] SOLZI M. *et al.*, *J. Mater. Chem.*, **21** (2015) 18331.
- [7] SVANSTRÖM S. *et al.*, *ACS Appl. Mater. Interfaces*, **12** (2010) 7212.
- [8] KLEIBERT A. *et al.*, *J. Phys.: Condens. Matter*, **20** (2008) 445005.
- [9] LLAMOSAS D. *et al.*, *Nanoscale*, **6** (2014) 13483.
- [10] AGRESTI A. *et al.*, *ACS Energy Lett.*, **4** (2019) 1862.
- [11] KATSIDIS C. and SIAPKAS D., *Appl. Opt.*, **41** (2002) 3978.
- [12] CALEFFI M. *et al.*, *Materials*, **19** (2021) 5507.
- [13] D’ADDATO S. *et al.*, *Beilstein J. Nanotechnol.*, **6** (2015) 404.
- [14] O’GRADY K. and BRADBURY A. *et al.*, *J. Magn. & Magn. Mater.*, **1** (1982) 91.
- [15] MANLEY P. *et al.*, *J. Phys. D: Appl. Phys.*, **47** (2014) 205301.
- [16] PALIK E., *Handbook of Optical Constants of Solids*, Vols. **1–4** (Academic Press) 1998.
- [17] CHING-PRADO E. *et al.*, *J. Mater. Sci. Mater. Electron.*, **29** (2018) 15299.
- [18] JELLISON G. and MODINE F., *Appl. Phys. Lett.*, **69** (2019) 371.
- [19] TOCCAFONDI C. *et al.*, *J. Phys. D: Appl. Phys.*, **47** (2014) 485301.
- [20] MAXWELL GARNETT J. C., *Philos. Trans. R. Soc. London A*, **203** (1904) 385.